

Electronic Supplementary Material (ESI)

This journal is © The Royal Society of Chemistry 2021

**Crystal structures and magnetic properties of one dimensional compounds constructed from Mn<sub>2</sub>(salen)<sub>2</sub> building block and organic selenite acid ligands**

Shao-Liang Zhang<sup>\*a</sup>, Xin-Chao Li<sup>a</sup>, Shi-Yu Gu<sup>a</sup>, Shi Guo<sup>a</sup>, Zi-Yu Liu<sup>a</sup>, Su-Yuan Zeng<sup>a</sup>, Shan-Shan Li<sup>b</sup>

<sup>a</sup>*Institution of Functional Organic Molecules and Materials, School of Chemistry and Chemical Engineering, Liaocheng University, Liaocheng, 252059, China*

<sup>b</sup>*School of Geography and Environment, Liaocheng University, Liaocheng, 252059, China*

E-mail: [zhangshaoliang05@163.com](mailto:zhangshaoliang05@163.com), zhangshaoliang@lcu.edu.cn

Supporting Information

**Table S1.** Selected bond lengths [ $\text{\AA}$ ] and angles [ $^\circ$ ] for complex **1**.

Complex <b>1</b>			
Mn(1)-O(3)	1.876(4)	Mn(2)-O(6)	1.879(4)
Mn(1)-O(4)	1.905(4)	Mn(2)-O(5)	1.866(4)
Mn(1)-N(1)	1.982(5)	Mn(2)-N(4)	1.989(5)
Mn(1)-N(2)	1.995(5)	Mn(2)-N(3)	1.973(5)
Mn(1)-O(1)	2.082(4)	Mn(2)-O(2)	2.064(4)
Mn(1)-O(4)#1	2.498(4)	Mn(2)-O(6)#2	2.922(4)
Se(1)-O(1)	1.681(4)	Se(1)-O(2)	1.681(4)
O(3)-Mn(1)-O(4)	95.52(18)	O(6)-Mn(2)-O(5)	92.78(18)
O(3)-Mn(1)-N(1)	91.8(2)	O(6)-Mn(2)-N(4)	89.7(2)
O(4)-Mn(1)-N(1)	165.8(2)	O(5)-Mn(2)-N(4)	162.4(2)
O(3)-Mn(1)-N(2)	172.6(2)	O(6)-Mn(2)-N(3)	165.0(2)
O(4)-Mn(1)-N(2)	89.7(2)	O(5)-Mn(2)-N(3)	91.9(2)
N(1)-Mn(1)-N(2)	82.1(2)	N(4)-Mn(2)-N(3)	81.7(2)
O(3)-Mn(1)-O(1)	96.56(19)	O(6)-Mn(2)-O(2)	96.58(19)
O(4)-Mn(1)-O(1)	94.88(18)	O(5)-Mn(2)-O(2)	97.5(2)
N(1)-Mn(1)-O(1)	96.4(2)	N(4)-Mn(2)-O(2)	99.5(2)
N(2)-Mn(1)-O(1)	88.2(2)	N(3)-Mn(2)-O(2)	96.9(2)
O(1)-Mn(1)-O(4)#1	172.74(16)	O(2)-Mn(2)-O(6)#2	178.74(6)

Symmetry code for complex **1**: -x, 2-y, 1-z; #2: -x, -y, -z

**Table S2.** Selected bond lengths [ $\text{\AA}$ ] and angles [ $^\circ$ ] for complex **2**.

Complex 2			
Mn(1)-O(3)	1.891(4)	Mn(2)-O(6)	1.873(4)
Mn(1)-O(4)	1.882(4)	Mn(2)-O(5)	1.910(4)
Mn(1)-N(1)	1.987(5)	Mn(2)-N(4)	1.976(5)
Mn(1)-N(2)	1.969(5)	Mn(2)-N(3)	1.997(5)
Mn(1)-O(1)	2.094(4)	Mn(2)-O(2)	2.095(4)
Mn(1)-O(3)#1	2.631(2)	Mn(2)-O(5)#2	2.523(2)
Se(1)-O(1)	1.711(3)	Se(1)-O(2)	1.689(4)
O(3)-Mn(1)-O(4)	95.07(18)	O(6)-Mn(2)-O(5)	95.32(18)
O(3)-Mn(1)-N(1)	89.3(2)	O(6)-Mn(2)-N(4)	91.9(2)
O(4)-Mn(1)-N(1)	169.2(2)	O(5)-Mn(2)-N(4)	165.98(19)
O(3)-Mn(1)-N(2)	165.6(2)	O(6)-Mn(2)-N(3)	170.3(2)
O(4)-Mn(1)-N(2)	91.3(2)	O(5)-Mn(2)-N(3)	89.53(19)
N(1)-Mn(1)-N(2)	82.3(2)	N(4)-Mn(2)-N(3)	81.7(2)
O(3)-Mn(1)-O(1)	95.91(17)	O(6)-Mn(2)-O(2)	96.62(18)
O(4)-Mn(1)-O(1)	95.72(17)	O(5)-Mn(2)-O(2)	95.76(17)
N(1)-Mn(1)-O(1)	93.59(18)	N(4)-Mn(2)-O(2)	95.33(18)
N(2)-Mn(1)-O(1)	96.32(19)	N(3)-Mn(2)-O(2)	91.24(18)
O(1)-Mn(1)-O(3)#1	174.9(8)	O(2)-Mn(2)-O(5)#2	172.42(7)

Symmetry code for complex **2**: 1-x, -y, -z; #2: 2-x, 1-y, -z

**Table S3** The parameters obtained by fitting Cole-Cole plot for **1**.

T / K	$\chi_s$	$\chi_t$	$\tau$	$a$
2.0	0.155	0.598	0.012264	0.14
2.2	0.162	0.662	0.002719	0.13
2.4	0.177	0.754	0.000710	0.11
2.6	0.211	0.887	0.000223	0.08
2.8	0.226	1.085	0.000077	0.05
3.0	0.000	1.386	0.000023	0.04

**Table S4** The parameters obtained by fitting Cole-Cole plot for **2**.

T / K	$\chi_{s,\text{tot}}$	$\Delta\chi_1$	$\tau_1$	$a_1$	$\Delta\chi_2$	$\tau_2$	$a_2$
2.0	0.0092	0.174	0.0000053	0.08	0.0248	0.0143680	0.29
2.2	0.0197	0.175	0.0000071	~0	0.0364	0.0051491	0.27
2.4	0.0002	0.174	0.0000048	~0	0.0213	0.0013606	0.41
2.6	0.0001	0.155	0.0000055	~0	0.0463	0.0000363	0.66
2.8	~0	0.145	0.0000091	~0	0.0678	0.0000003	0.83
3.0	~0	0.161	0.0000076	~0	0.0707	0.0000005	0.91

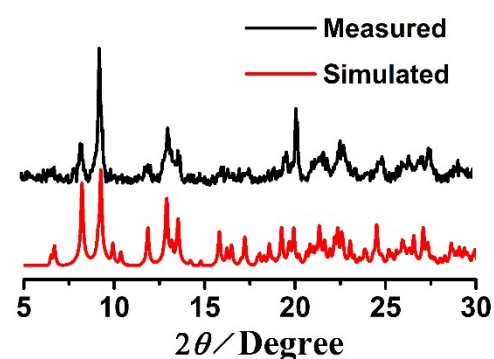


**Figure S1.** The powder XRD pattern of **1** in black and its simulation in red.

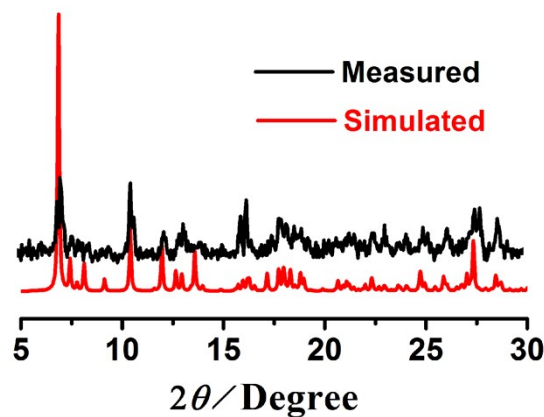


**Figure S2.** The powder XRD pattern of **2** in black and its simulation in red.

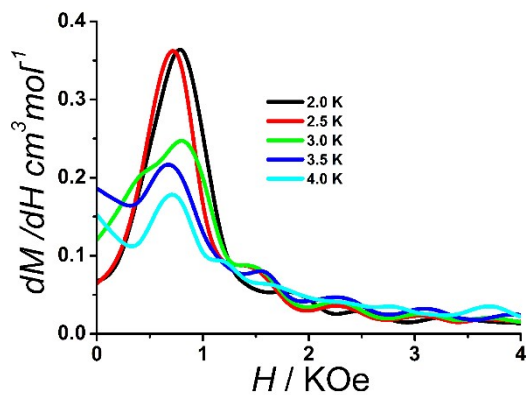


**Figure S3.** The derivative of field-dependent magnetization of **1** measured at different temperatures.

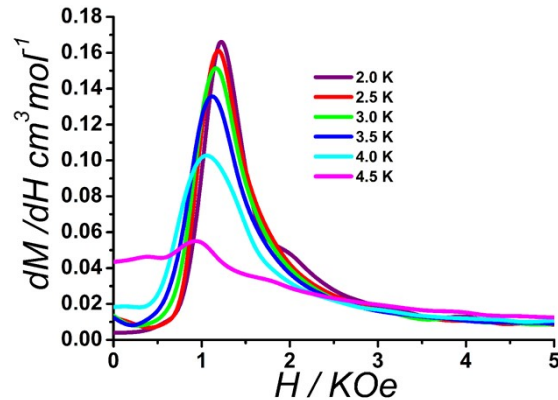


**Figure S4.** The derivative of field-dependent magnetization of **2** measured at different temperatures.

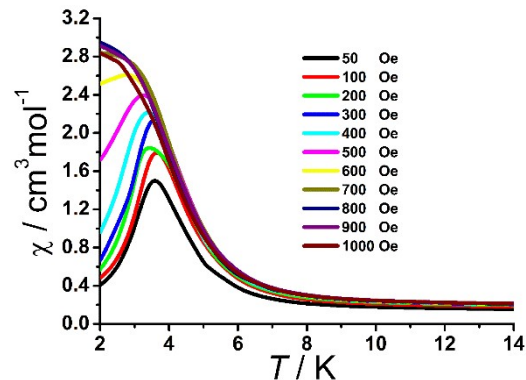


**Figure S5** The  $\chi_M$  versus  $T$  plots measured at different external fields of **1**.

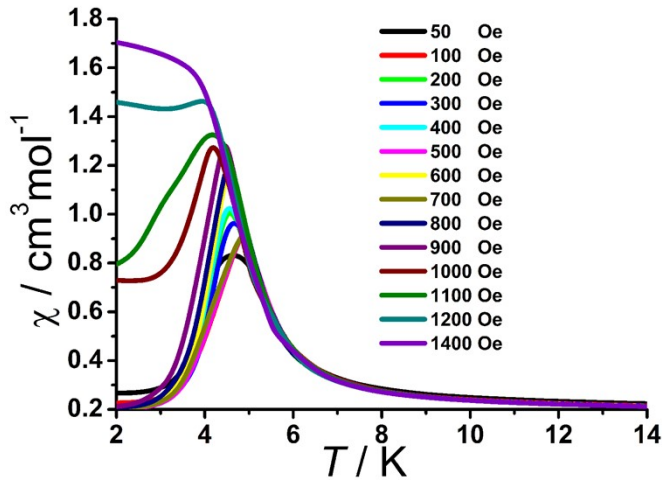


**Figure S6** The  $\chi_M$  versus  $T$  plots measured at different external fields of **2**.

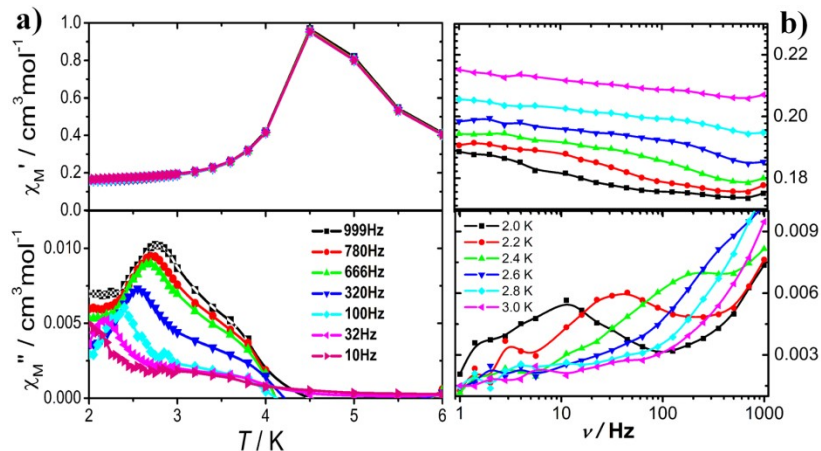


**Figure S7.** Variable-temperature (a) and variable-frequency (b) *ac* magnetic susceptibility data of **2** under  $H_{ac} = 2$  Oe and  $H_{dc} = 0$  Oe.

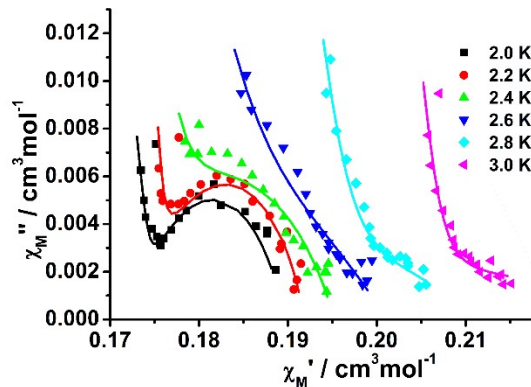


**Figure S8.** Cole–Cole plots of the compound **2** from 2.0 to 3.0 K. The solid lines represent the fitting using the generalized Debye model

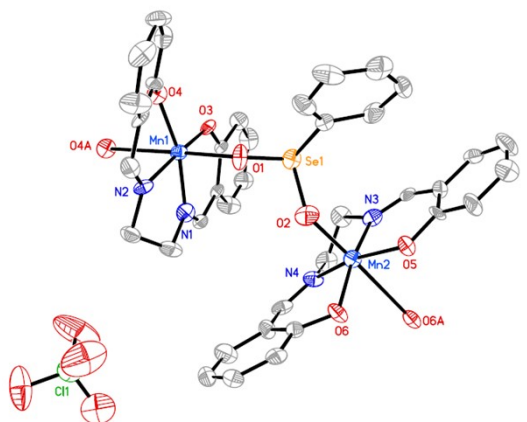


**Figure S9** The asymmetric unit of complex **1**, rendered with 30% probability ellipsoids. Hydrogen atoms are omitted for clarity.

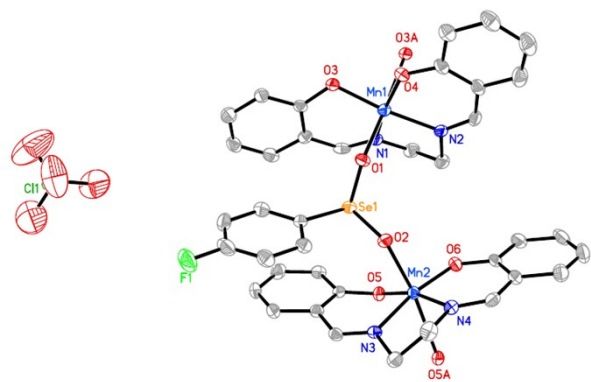


**Figure S10** The asymmetric unit of complex **2**, rendered with 30% probability ellipsoids. Hydrogen atoms are omitted for clarity.